Design and Magnetic Field Uniformity of Giant Magnetostrictive Ultrasonic Transducer for Progressive Sheet Forming

LI Pengyang[1,2*], *LIU Qiang*[1,2], *ZHOU Xuan*[1,2], *LI Wei*[1,2], *WANG Limeng*[1,2]

1. The Ministry of Education Key Laboratory of NC Machine Tools and Integrated Manufacturing Equipment, Xi'an University of Technology, Xi'an 710048, P. R. China;
2. Key Laboratory of Manufacturing Equipment of Shaanxi Province, Xi'an University of Technology, Xi'an 710048, P. R. China

(Received 17 August 2019; revised 3 January 2020; accepted 27 May 2020)

Abstract: Design of a giant magnetostrictive ultrasonic transducer for progressive sheet forming was presented. A dynamic analysis of the theoretically designed ultrasonic vibration system was carried out using the finite element method (FEM). In addition, simulations were performed to verify the theoretical design. Then, a magnetically conductive material was added between the giant magnetostrictive rod and the permanent magnet. Besides, magnetic field simulations of the transducer were performed. The influence of the material thickness of the magnetically conductive material on uniformity of the induced magnetic field was studied. Furthermore, the impedance analysis and amplitude measurement were performed to compare the performance of transducers with and without the magnetically conductive material. The experimental results show that the magnetic field uniformity is the highest when the magnetically conductive material has a thickness of about 1.6 mm. The output amplitude of the giant magnetostrictive transducer is improved by adding the magnetically conductive material. Moreover, the mechanical quality factor and impedance are reduced, while the transducer operates more stably.

Key words: giant magnetostrictive material (GMM); ultrasonic transducer; magnetic field uniformity; finite element analysis

CLC number: TB663 **Document code:** A **Article ID:** 1005-1120(2020)03-0393-10

0 Introduction

Ultrasonic vibration-assisted sheet forming is the progressive forming of ordinary sheet material with the addition of ultrasonic vibrations to improve the process. During sheet forming, the metallic material undergoes plastic deformation, however, adopting ultrasonic vibrations that periodically change direction can significantly reduce the flow stress required for plastically deforming the material, thereby improving the forming limit of the material and the quality of the finished product[1]. After applying ultrasonic vibrations to the sheet, the average axial force can reduce by 23.5%, and the rebound and surface roughness can also reduce[2]. Hou et al.[3] carried out a comparative experiment of laminated drilling with three methods of conventional drilling, rotary ultrasonic assisted drilling and low frequency vibration assisted drilling. Compared with the conventional drilling, the introductions of rotary ultrasonic and axial low frequency vibration can reduce drilling temperature and improve drilling quality.

At present, piezoelectric ceramics are widely used in machining as materials for ultrasonic transducers. However, several disadvantages such as the

*Corresponding author, E-mail address: lipengyang@xaut.edu.cn.

How to cite this article: LI Pengyang, LIU Qiang, ZHOU Xuan, et al. Design and magnetic field uniformity of giant magnetostrictive ultrasonic transducer for progressive sheet forming[J]. Transactions of Nanjing University of Aeronautics and Astronautics, 2020, 37(3): 393-402.

http://dx.doi.org/10.16356/j.1005-1120.2020.03.006

low power density of piezoelectric ceramics, frequent overheating failures, and fragility of the material have limited large-scale application of piezoelectric ceramics in high power applications. To this end, giant magnetostrictive material (GMM) offer several advantages including a large magnetostriction coefficient, high power capacity, and fast response speed, thus becoming research focus in the development of high-power and large-amplitude ultrasonic processing systems[4-5].

A number of studies have recently been carried out on magnetostrictive materials. Jammalamadaka et al.[6] developed and tested a 100 kHz giant magnetostrictive transducer for detecting defects in concrete structures using ultrasonic transmission technique. Karunanidhi et al.[7] designed a magnetostrictive actuator for a high dynamic servo valve and found that valves with magnetostrictive actuators have a faster time response compared with conventional servo valves. In addition, their results suggest that the valve has good static and dynamic characteristics and is suitable for high speed drive systems.

To test magnetostrictive materials, Zhao et al.[8] designed a test analysis system. They used giant magnetostrictive materials and analyzed the nonlinear hysteresis characteristics using theoretical methods, meanwhile, they studied the effects of damping, prestress and spring stiffness on the maximum amplitude. Sheykholeslami et al.[9] conducted an experimental comparison of the first and second longitudinal modes of a giant magnetostrictive transducer. In their analysis, they demonstrated a higher quality factor of the second mode of the ultrasonic transducer, while sensitivity of the Young's modulus was lower. Furthermore, they examined the variation in Young's modulus (ΔE effect) of the GMM rod using both theory and experiments[10].

Mathematical models and numerical simulations have been previously used to study GMM. Zeng et al.[11] analyzed the magnetic energy conversion and vibration characteristics of magnetostrictive power ultrasonic transducers by establishing a mathematical model of the transducer vibrator and performing computer simulations. Zhu et al.[12] also used a theoretical approach to develop an accurate giant magnetostrictive actuator with a thermal displacement suppression system. The thermal displacement control mechanism consisted of a temperature control module and a thermal displacement compensation module and the system significantly improved the output characteristics of the giant magnetostrictive drive, especially the displacement accuracy. Zheng et al.[13] established a dynamic model of the radiant panel of the magnetostrictive transducer under the action of the magnetostrictive rod through a spring and discussed the effect of its stiffness, positioned between the magnetostrictive rod and the radiant panel, on the amplitude of the radiant panel. By selecting a spring with suitable properties, the magnetostrictive rod can be prestressed, thus, providing the system with the dynamic characteristics required for vibration and allowing large displacement of the radiant panel.

Wang et al.[14] proposed a giant magnetostrictive actuator based on permanent magnets. The use of permanent magnets to drive the magnetic field of magnostrictive Terfenol-d can inhibit temperature effects associated with the skin effect caused by eddy currents of the solenoid.

While GMM are widely used in the fields of ultrasonic chemistry, industrial processing, and medicine[15], current studies on GMM are mainly focused on low frequency systems and detection devices. For example, the high-frequency magnetostrictive transducers are widely used for ultrasonic detection; however, giant magnetostrictive power ultrasonic transducers are still rarely used in machining.

Li et al.[16] studied the geometry of the coil and the influence of magnetic circuit components on the magnetic field characteristics and output displacement of the transducer. They showed that installing a soft-iron core at both ends of the GMM rod can increase the magnetic field strength, reduce magnetic flux leakage, and increase the transduction of the output shift, while reducing the drive current. Cai et al.[17] studied the influence of different material prop-

erties of the magnetizer on the vibration performance of an ultrasonic system. Highly permeable ferrite can improve the electromechanical energy conversion efficiency of low-power ultrasonic vibration system; whereas high-power ultrasonic vibration systems must take into account the magnetic permeability rate and saturation flux density, allowing the magnetizer to operate in a non-magnetic saturation state to improve system conversion efficiency.

Permanent magnets are typically placed at both ends of the GMM rod to generate the bias magnetic field of the giant magnetostrictive transducer. However, the magnetic field distribution in the GMM rod will be non-uniform, owing to the low magnetic permeability of permanent magnets, which limits the performance of the giant magnetostrictive transducer. Adding a highly permeable magnetic conductive material between the permanent magnet and GMM rod of the giant magnetostrictive transducer can create a more uniform magnetic field distribution in the GMM rod[18-19], but further research of the magnetic conductive material influence on the giant magnetostrictive transducer is needed.

In this paper, a theoretical design of a novel giant magnetostrictive ultrasonic transducer was presented. Dynamics of the ultrasonic vibration device was analyzed by using finite element analysis and the transducer was experimentally tested. Further, a magnetically conductive material (electrician pure iron) of various thicknesses was placed between the GMM rod and the permanent magnet to study the influence of thickness on the axial magnetic field uniformity. Finally, performances of transducers with or without magnetically conductive materials were compared.

1 Structural Design of Ultrasonic Transducer

1.1 Principle analysis of ultrasonic transducer

Fig.1 shows a schematic illustration of the proposed giant magnetostrictive ultrasonic vibration device. The ultrasonic generator produces a high-frequency electrical signal that is transmitted from the primary winding of the non-contact power transmission device to the secondary winding and through the lead wire to the excitation coil of the GMM rod. Then, the excitation coil generates a high-frequency alternating magnetic field, and the GMM rod generates high-frequency magnetostriction under an alternating magnetic field and the ultrasonic vibrations are amplified through the horn and transmitted to the tool head.

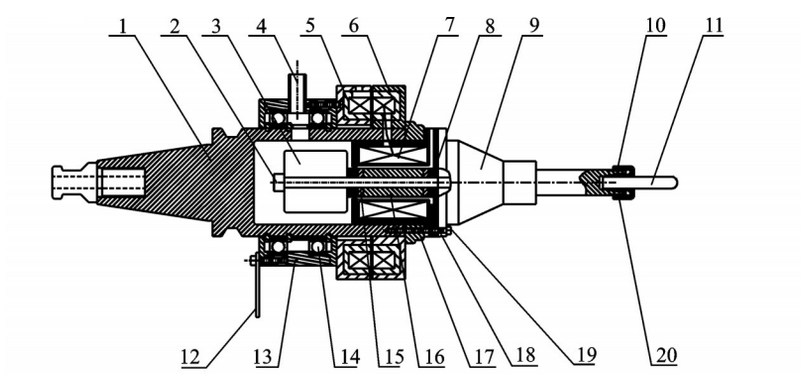

1—Shank; 2—Pre-tightening bolt; 3—Rear cover; 4—Intake pipe; 5—Primary winding; 6—Secondary winding; 7—Coil; 8—Magnetic conductive block; 9—Luff; 10—Elastic chuck; 11—Horn; 12—Stopper; 13—Housing; 14—Bearing; 15—Permanent magnet; 16—GMM rod; 17—Magnetic cylinder; 18—Magnetic sheet; 19—Screw; 20—Nut

Fig.1 Schematic of ultrasonic vibration device

GMM rod is a brittle material with a tensile strength of about 28 MPa. Therefore, an appropriate prestress must be applied to the GMM rod in order to reduce tensile stress under actual working conditions. Moreover, adopting a certain amount of prestress can increase the magnetostriction coeffi-

cient[20]. Thus, pre-tightening bolts are applied a suitable prestress to the GMM rod.

In this study, the rear cover, magnetic conductive block, permanent magnet, GMM rod and horn were connected by a bolt, made of non-magnetic stainless steel. Cylindrical permanent magnets were placed at both ends of the GMM rod. The shank, a magneticallly conductive material, and horn were fixed by screws. Finally, a quarter-wavelength conical transition step-type composite horn was designed to reduce the longitudinal length of the ultrasonic vibration device.

1.2 Composite ultrasonic vibrator design

The front and rear cover plates of the vibrator and GMM can be regarded as continuous elastic media. Thus, elastic equations were established for each and the boundary conditions were used to obtain various design parameters. Fig.2 shows a one-dimensional segment within a variable section of the vibrator body, where the axis of symmetry is the x-axis and tensile stress acting on the segment defined by a small-volume element $(x, x + \mathrm{d}x)$ is $\sigma_x \mathrm{d}x$.

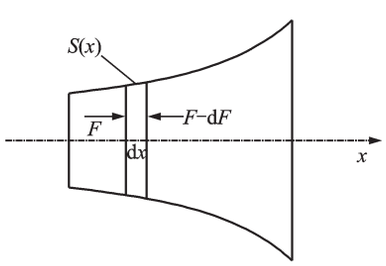

Fig.2 One-dimensional segment of a variable section of the vibrator body

According to Newton's laws, the kinetic equation can be written as

$$\frac{\partial(S\cdot\sigma)}{\partial x}\mathrm{d}x = S\cdot\rho\frac{\partial^2\xi}{\partial t^2}\mathrm{d}x \tag{1}$$

where σ is the stress function and $\sigma=\sigma(x)E\dfrac{\partial\xi}{\partial x}$, here E is the Young's modulus; S is the function of the cross-sectional area of the rod and $S = S(x)$; ξ is the particle displacement function and $\xi=\xi(x)$; and ρ is the density of the rod material.

When the rod performs a simple harmonic motion, $\xi(x,t)=\xi(x)\mathrm{e}^{\mathrm{j}\omega t}$, the equation for the simple harmonic vibration state of the variable section rod can be obtained as

$$\frac{\partial^2\xi}{\partial x^2}+\frac{1}{S}\cdot\frac{\partial S}{\partial x}\cdot\frac{\partial\xi}{\partial x}+k^2\xi(x)=0 \tag{2}$$

where k is the number of circular waves and $k = \omega/c$, here c is the speed of sound inside the member and $c = (E/\rho)^{1/2}$.

The velocity of vibration, $V = \mathrm{j}\omega\xi$, was substituted into Eq.(2) to obtain the vibration velocity equation for longitudinal vibration of the variable cross section bar

$$\frac{\partial^2 V}{\partial x^2}+\frac{1}{S(x)}\cdot\frac{\partial S}{\partial x}\cdot\frac{\partial V}{\partial x}+k^2V=0 \tag{3}$$

If the cross section of the bar is uniform and S is the constant, Eq.(3) can be simplified as

$$\frac{\partial^2 V}{\partial x^2}+k^2V=0 \tag{4}$$

The general solution to the equations of vibration velocity and force of a body with a uniform cross section is

$$V(x)=A\sin kx+B\cos kx \tag{5}$$

$$F(x)=\frac{ES}{\mathrm{j}\omega}\frac{\partial V}{\partial x}=-\mathrm{j}Z(A\cos kx-B\sin kx) \tag{6}$$

where Z is the characteristic acoustic impedance of the vibrator and $Z=\rho cS$.

The magnetic conductive material outside the coil and the coil does not participate in the vibration, therefore, the ultrasonic vibrator can be simplified as a rear cover, two magnetic conductive blocks, a GMM rod and a horn, as shown in Fig.3. The nodal plane is located at the joint surface between the horn and the magnetic conductive block. The front surface vibration velocity of the transducer vibrator is V_f and the elastic force $F=-Z_\omega V_f$, where Z_ω is the input impedance of the front surface of the transducer. Ends of the vibrator are in a free state, so $F_1=F_8=0$. Furthermore, the velocity of the particle at the nodal plane is zero, thus $V_4(l_4)=V_5(0)=0$.

On the left-hand-side (LHS) of the section, the boundary conditions are

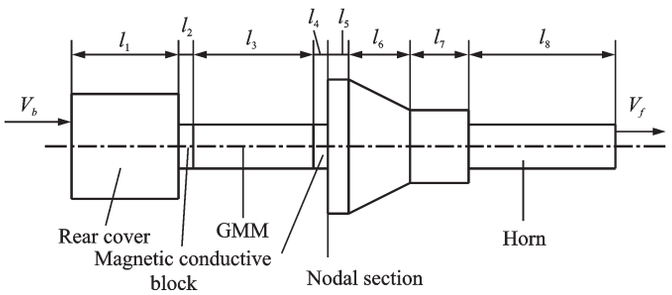

Fig.3 Simplified ultrasonic vibrator

$$\begin{cases} V_1(0)=V_b & F_1(0)=0 \\ V_1(l_1)=V_2(0) & F_1(l_1)=F_2(0) \\ V_2(l_2)=V_3(0) & F_2(l_2)=F_3(0) \\ V_3(l_3)=V_4(0) & F_3(l_3)=F_4(0) \\ V_4(l_4)=0 & F_4(l_4)=F_5(0) \end{cases} \tag{7}$$

According to the boundary conditions and general solutions of the vibration velocity and force equations, the frequency equations on LHS of the nodal plane can be obtained as

$$\frac{Z_1}{Z_2}\tan(k_1l_1)\tan(k_2l_2)+\frac{Z_1}{Z_3}\tan(k_1l_1)\tan(k_3l_3)+\frac{Z_1}{Z_4}\tan(k_1l_1)\tan(k_4l_4)+\frac{Z_2}{Z_3}\tan(k_2l_2)\tan(k_3l_3)+\frac{Z_2}{Z_4}\tan(k_2l_2)\tan(k_4l_4)=1 \tag{8}$$

On the right-hand-side (RHS) of the section, the boundary conditions are

$$\begin{cases} V_5(0)=0 & F_5(0)=F_4(l_4) \\ V_5(l_5)=V_6(0) & F_5(l_5)=F_6(0) \\ V_6(l_6)=V_7(0) & F_6(l_6)=F_7(0) \\ V_7(l_7)=V_8(0) & F_7(l_7)=F_8(0) \\ V_8(0)=V_f & F_8(l_8)=0 \end{cases} \tag{9}$$

Dimensions of the various parts of the transducer assembly are determined from Eq.(8) and Eq.(9) by using known parameters. The rear cover of the transducer is primarily used to achieve unobstructed unidirectional radiation, ensuring minimal energy loss through the rear surface of the transducer, thereby increasing the forward radiated ultrasonic power.

In general, the rear cover of a transducer is constructed from some types of heavy metals. If the rear cover is completely comprised of heavy metals, the total mass of the transducer and rotational moment of inertia increases, which can affect the performance of the vibration system[21-22]. However, combining non-magnetic 316 stainless steel and an aluminum alloy can limit the radiation of energy from the rear cover, and also reduce the quality of the transducer.

Since the diameter of the magnetic conductive block is much smaller than that of the large end of the horn, the magnetic conductive block was designed in a stepped shape in order to reduce the impedance. The rear cover and horn were made of 316 non-magnetic stainless steel to avoid magnetic leakage from the transducer. Properties of the selected materials are listed in Table 1.

Table 1 Material properties

Material	Density / (kg•m^{-3})	Poisson's ratio	Young's modulus / GPa
316 stainless steel	8 000	0.28	193.0
Aluminum	2 790	0.34	71.5
GMM	9 250	0.30	27.5
Pure iron	7 860	0.29	195.0

The length of the transducer: $l_2=l_4=4.5$ mm, $l_3=42$ mm, $l_5=10$ mm, $l_6=21$ mm, $l_7=20$ mm. Diameter: $D_1=35$ mm, $D_2=D_3=D_4=15$ mm, $D_5=49$ mm, $D_7=25$ mm, $D_8=15$ mm.

Substituting the above parameters into Eq.(8) and solving Eq.(9) yield equations for l_5, l_6, l_7, and l_8, which can be solved in MATLAB to obtain values for l_1 and l_8: $l_1=36.5$ mm, $l_8=51.7$ mm.

In theory, the length of the tool bar should be selected according to the half-wavelength theory. However, in actual production, the length of the tool bar is usually less than 1/4 wavelength and the lateral dimension is less than 1/10 wavelength,

thus, enhancing rigidity of the tool. Furthermore, resonance of the whole system at the working frequency reduces; the length of the end of the original variable amplitude also appropriately shortens. The length is related to the equivalent quality of the tool, while it can be approximated using the following equations[23]

$$\Delta l = \frac{M_t}{\rho S} \tag{10}$$

$$M_t = \frac{\tan(k_t l_t)}{k_t l_t} m_t \tag{11}$$

$$m_t = \rho_t l_t S_t \tag{12}$$

where M_t is the tool equivalent mass, ρ the end horn density, S the end horn face area, m_t the tool bar actual mass, k_t the round wave number, ρ_t the density of the tool bar, and l_t the length of the tool bar.

The tool is made of steel, designed for high-speed tools. Diameter D_t=7 mm and length l_t=20 mm were obtained for the tool head

$$l_8 = 51.7 - 5 = 46.7 \text{ (mm)}$$

2 Finite Element Analysis of Transducer

2.1 Modal analysis of ultrasonic transducer

A modal analysis of the transducer was performed in ANSYS using the piezoelectric-compressive magnetic comparison method. The pre-tightening bolt was simplified and the rear cover was considered a unified body. The SOLID95 element was selected for the front and rear cover plates as well as the magnetic conductive block. In the coupled field analysis, the SOLID98 element was adopted for the piezoelectric ceramic[24]. Therefore, the SOLID98 element was also selected for the GMM rod.

The frequency range was set to 16—24 kHz and the Lanczos method was used to perform the calculations. During post-processing, the required longitudinal vibration mode frequency is 19.65 kHz and the vibration mode of the transducer is shown in Fig.4. The vibration output at the top of the horn is the largest, while the vibration at the back cover plate and the flange of the horn is relatively small. The natural frequency of the transducer is very close to the design frequency (20 kHz), which basically verifies the correctness of the theoretical design.

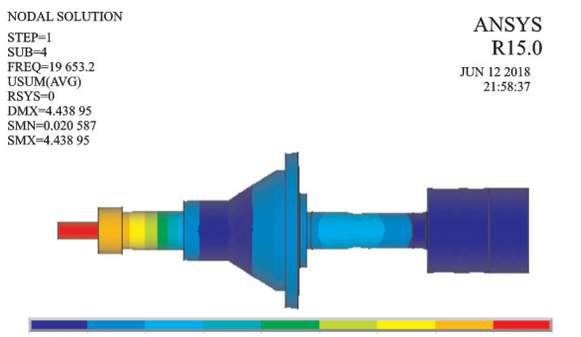

Fig.4 Transducer vibration mode

2.2 Magnetic field analysis of transducer

A static magnetic field analysis of the transducer was performed in ANSYS using the two-dimensional (2-D) symmetrical PLANE13 element. Because of the large longitudinal size of the front cover plate and the rear cover plate, the effect on the magnetic field is small. Therefore, only a part of the model is established. Magnetic permeability of each material is listed in Table 2 and the finite element model of the transducer is shown in Fig.5.

Table 2 Relative magnetic permeability of different materials

Material	GMM	Permanent magnet	Pure iron	Hard aluminum
Relative permeability	10	1.07	2 000	1

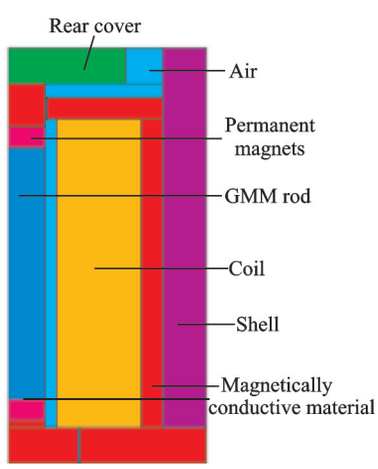

Fig.5 Finite element model of transducer

Since GMM is relatively brittle, non-uniformity of the internal magnetic field generates internal stress that can reduce the service life of the materials. Thus, realizing a uniform magnetic field distribution of the GMM rod during expansion and contraction can improve the performance of the transducer, and increasing uniformity of the internal magnetic field is important.

Simulations were carried out with a magnetically conductive material of various thicknesses between the permanent magnet and the GMM rod. The magnetic field intensity distribution in the axial direction of the GMM rod is shown in Fig.6. Thickness values of the guide can be calculated[25] and when the magnetic sheet is used, the axial magnetic field uniformity of the GMM rod is

$$\eta = \frac{\sum_{i=1}^{n} \frac{H_i}{n}}{H_{\max}} \times 100\% \tag{13}$$

where H_i is the magnetic field strength of the ith point on the GMM rod, n the number of points considered, and $H_{\max}$ the maximum magnetic field strength in the GMM rod.

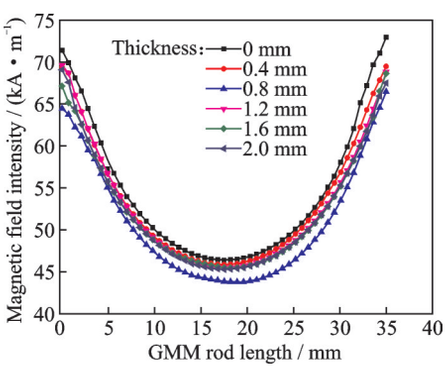

Fig.6 Axial magnetic field intensity distribution in GMM rod

Fig.7 shows the axial magnetic field uniformity of the GMM rod at various thicknesses of magnetically conductive material. When the magnetically conductive material is added between the permanent magnet and the GMM rod, the magnetic field uniformity in the GMM rod improves. Moreover, the highest uniformity was obtained with a magnetic conductive material thickness of about 1.6 mm. Above 1.6 mm, the magnetic field uniformity decreases. Therefore, to improve energy conversion efficiency, the length of the GMM rod should increased as much as possible, such that the thickness of the magnetically conductive material minimizes.

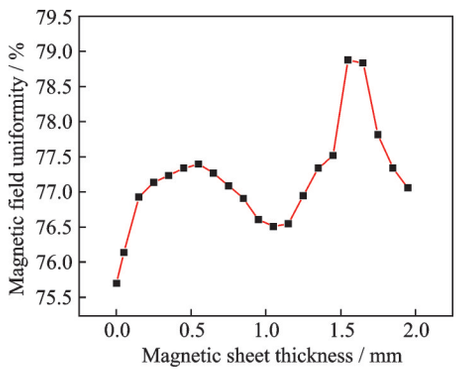

Fig.7 Magnetic field uniformity of GMM rod

3 Experimental Procedure

The theoretical design and simulation analysis were validated by experimentally measuring the resonant frequency and amplitude of the ultrasonic transducer. A prototype of the giant magnetostrictive ultrasonic vibration device was fabricated, as shown in Fig.8. The experimental measurement system consists of a high-speed bipolar power supply (BP4620) to generate voltage signals of different frequencies and amplitudes, an impedance analyzer to measure the impedance of the transducer, and a laser oscillator used to measure the amplitude of the transducer close to the resonant frequency.

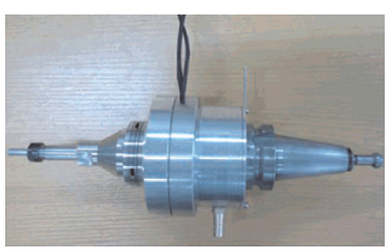

Fig.8 Prototype of giant magnetostrictive ultrasonic vibration device for progressive sheet forming

The effect of magnetically conductive material between the GMM rod and the permanent magnet on the performance of the giant magnetostrictive transducer was studied, while the validity of simulation analysis was verified. According to Fig.7, the magnetic field uniformity is the highest when the

thickness of the magnetic conductive material is about 1.6 mm. Therefore, the thickness of the magnetically conductive material was set to 1.6 mm in subsequent experiments.

Impedance analysis was performed to compare the results of the magnetostrictive transducer with or without the additional magnetic material. The mechanical quality factor decreases, as shown in Table 3, after the magnetically conductive material is added to the giant magnetostrictive transducer.

Table 3 Results of impedance analysis of giant magnetostrictive transducer

Magnetic material	Resonant frequency f_s	Half power point frequency		Mechanical quality factor Q_m
		f_a	f_b	
Without	19.25	19.20	19.29	200.52
With	19.23	19.15	19.28	147.9

Figs.9 and 10 show impedance circles of the giant magnetostrictive transducer without and with the magnetically conductive material, respectively. It can be observed that the impedance decreases when the magnetically conductive material is added.

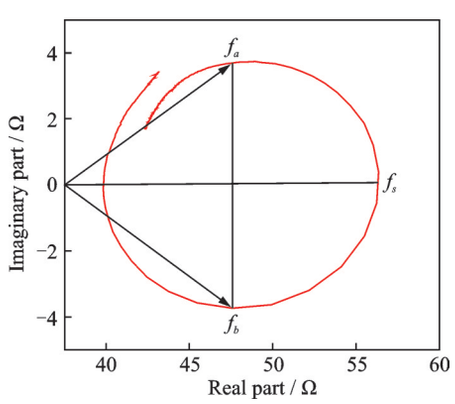

Fig.9 Impedance circle without magnetically conductive material

Fig.11 shows the amplitude of the top of the transducer tool head at different frequencies. The test conditions were as follows: Voltage of 60 V, square waveform, and the frequency varied from 19.0 kHz to 19.6 kHz, with a step size of 50 Hz. The output amplitude of the transducer with and without magnetically conductive material is measured three times at each frequency point, and then the average value is obtained.

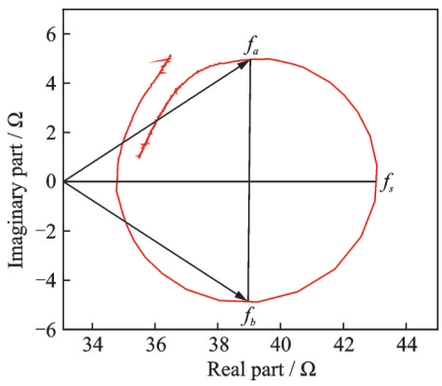

Fig.10 Impedance circle with magnetically conductive material

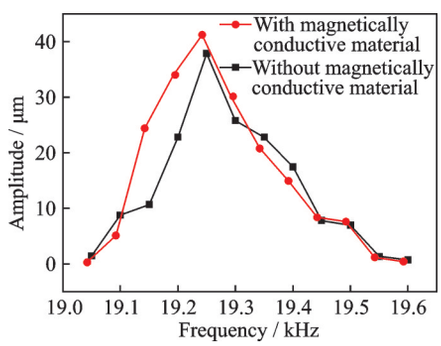

Fig.11 Transducer amplitude at different frequencies

The results show that the maximum amplitude of the giant magnetostrictive transducer is 37.86 μm. However, when the magnetically conductive material is placed between the GMM rod and the permanent magnet, the maximum amplitude of the giant magnetostrictive transducer increases to 41.24 μm. In conclusion, the maximum amplitude of the transducer increases when a magnetically conductive material is added between the GMM rod and the permanent magnet.

4 Conclusions

The theoretical design of a giant magnetostrictive ultrasonic transducer was presented. Finite element analysis was performed to analyze the dynamics of the ultrasonic vibration system. Then a prototype of the giant magnetostrictive ultrasonic vibration device was fabricated and an impedance analysis of the transducer was performed. Amplitude measurements show that the actual resonant fre-

quency of the transducer is 19.25 kHz and the maximum amplitude of the transducer is 37.86 μm, thus validating the theoretical design and simulation.

Furthermore, a magnetic field analysis of the giant magnetostrictive transducer was carried out. Adding a magnetically conductive material, comprised of pure iron between the GMM rod and the permanent magnet, resulted in a more uniform magnetic field, improved the utilization ratio of the GMM rod, and achieved transduction. In addition, the overall working performance of the device was more stable. Moreover, the magnetic field uniformity of the GMM rod was the highest when the thickness of the magnetic conductive material was about 1.6 mm.

Performance of the giant magnetostrictive transducer with and without the magnetically conductive material was compared. The results show that the addition of the magnetically conductive material reduces the mechanical quality factor and impedance of the giant magnetostrictive transducer and increases the maximum amplitude. This work has great significance to the optimal design of high-power and large-amplitude ultrasonic transducers.

References

[1] PETRUZELKA J, SARMANOVA J, SARMAN A. The effect of ultrasound on tube drawing[J]. Journal of Materials Processing Technology, 1996, 60(1/2/3/4): 661-668.

[2] VAHDATI M, MAHDAVINEJAD R, AMINI S. Investigation of the ultrasonic vibration effect in incremental sheet metal forming process[J]. Proceedings of the Institution of Mechanical Engineers Part B Journal of Engineering Manufacture, 2015, 231(6): 1-12.

[3] HOU Shujun, GAO Xiaoxing, LI Kai, et al. Vibration assisted drilling of carbon fiber reinforced plastic and titanium stacks[J]. Journal of Nanjing University of Aeronautics & Astronautics, 2018, 50(3): 295-301. (in Chinese)

[4] OLABI A G, GRUNWALD A. Design and application of magnetostrictive materials[J]. Materials & Design, 2008, 29(2): 469-483.

[5] LIU W J, ZHOU L S, XIA T J, et al. Rare earth ultrasonic transducer technique research[J]. Ultrasonics, 2006, 44(4): 689-692.

[6] JAMMALAMADAKA S N, MARKANDEYULU G, KANNAN E. Development of a magnetostrictive transducer for nondestructive testing of concrete structures[J]. Applied Physics Letters, 2008, 92(4): 044102-1-044102-3.

[7] KARUNANIDHI S, SINGAPERUMAL M. Design, analysis and simulation of magnetostrictive actuator and its application to high dynamic servo valve[J]. Sensors and Actuators, A: Physical, 2010, 157(2): 185-197.

[8] ZHAO T Y, YUAN H Q, PAN H G, et al. Study on the rare-earth giant magnetostrictive actuator based on experimental and theoretical analysis[J]. Journal of Magnetism & Magnetic Materials, 2018, 460(8): 509-524.

[9] SHEYKHOLESLAMI M R, HOJJAT Y, GHODSI M, et al. Comparative discussion between first and second modes of Terfenol-D transducer[C]//Proceedings of Sensors and Smart Structures Technologies for Civil, Mechanical, and Aerospace Systems 2015.[S. l.]: International Society for Optics and Photonics, 2015.

[10] SHEYKHOLESLAMI M R, HOJJAT Y, GHODSI M, et al. Investigation of ΔE effect on vibrational behavior of giant magnetostrictive transducers[J]. Shock and Vibration, 2015, 2015: 1-9.

[11] ZENG G, CAO B, ZENG H Q. Analysis of dynamic characteristics of the magnetostrictive power ultrasonic transducer[J]. Applied Mechanics and Materials, 2012, 105(1): 1693-1696.

[12] ZHU Y C, JI L. Theoretical and experimental investigations of the temperature and thermal deformation of a giant magnetostrictive actuator[J]. Sensors and Actuators, A: Physical, 2014, 218: 167-178.

[13] ZHENG Rongyue, HUANG Yan, LIN Wenfeng. Free vibration analysis of a box orthotropic rectangular plate structure[J]. Journal of Vibration and Shock, 2009, 28(3): 164-167. (in Chinese)

[14] WANG L, TAN J B, ZHANG S. A giant magnetostrictive actuator based on use of permanent magnet[J]. International Journal of Advanced Manufacturing Technology, 2010, 46(9/10/11/12): 893-897.

[15] LIU Huifang, WANG Shijie, ZHANG Yu, et al. Study on the giant magnetostrictive vibration-power generation method for battery-less tire pressure monitoring system[J]. Journal of Mechanical Engineering Science, 2015, 229(9): 1639-1651.

[16] LI Mingfan, XIANG Zhanqin, LV Fuzai. Magnet circuit design and optimization of giant magnetostrictive transducer[J]. Journal of Zhejiang University (Engi-

neering Science), 2006, 40(2): 192-196. (in Chinese)

[17] CAI Wanchong, ZHANG Jianfu, YU Dingwen, et al. Equivalent amplitude model for a giant magnetostrictive transducer based on unsteady electromechanical conversion coefficient[J]. Journal of Mechanical Engineering, 2017, 53(19): 52-58. (in Chinese)

[18] HE X P. Active vibration device of rare earth giant magnetostrictive ultrasonic transducer: China, 200420041835.3[P]. 2005-04-13.

[19] CHEN Hao, TANG Yongning, GU Zhengqiang. Design of a giant magnetostrictive tonpilz transducer[J]. Rader & ECM, 2015(3): 60-64. (in Chinese)

[20] CALKINS F T, DAPINO M J, FLATAU A B. Effect of prestress on the dynamic performace of a terfenol-d transducer[C]//Proceedings of Smart Structures and Materials 1997: Smart Structures and Integrated Systems. [S.l.]: International Society for Optics and Photonics, 1997, 3041: 293-304.

[21] LIN Zhongmao. Principle and design of ultrasonic horn [M]. Beijing: Science Press, 1987. (in Chinese)

[22] DONG Huijuan, YUE Tong, ZHANG Guanyu. Study on half-wave ultrasonic vibration system suitable for micropore[J]. Electromachining & Mould, 2004(4): 33-35. (in Chinese)

[23] ZHANG Kexin, ZHANG Xianghui, GAO Ju. Ptimum design of acoustic horns with tool for ultrasonic machining using finite-element analysis[J]. Machinery Design & Manufacture, 2011(11): 33-35. (in Chinese)

[24] PARRINI L. New technology for the design of advanced ultrasonic transducers for high-power applications[J]. Ultrasonics, 2003, 41(4): 261-269.

[25] LI Pengyang, LIU Qiang, ZHOU Lingxia. Design and numerical simulation analysis of a giant magnetostrictive ultrasonic transduce[J]. Journal of Basic Science and Engineering, 2017, 25(5): 1065-1075. (in Chinese)

Acknowledgements This work was supported by the National Science Foundation of China (No.51675422), and the Shaanxi Province Key Research and Development Plan Project of China (No.2017GY-028)

Author Prof. **LI Pengyang** received the B.S. degree in mechanical engineering in 2002 from Xi'an University, and received the Ph.D. degree in computer science and technology in 2010 from Northwestern Polytechnical University. He is currently a professor of School of Mechanical and Precision Instrument Engineering, Xi'an University of Technology. His research interests include ultrasonic vibration machining, machining process monitoring, machine tool interface, etc.

Author contributions Prof. **LI Pengyang** designed the study, complied the models. Mr. **LIU Qiang** designed the giant magnetostrictive ultrasonic transducer, conducted the annlysis, interpreted the results. Mr. **ZHOU Xuan** completed the experiments. Mr. **LI Wei** wrote the manuscript. Ms. **WANG Limeng** contributed to the discussion and background of the study. All authors commented on the manuscript draft and approved the submission.

Competing interests The authors declare no competing interests.

(Production Editor: XU Chengting)

板料渐进成形超磁致伸缩超声换能器设计及磁场均匀度研究

李鹏阳[1,2], 刘 强[1,2], 周 玄[1,2], 李 伟[1,2], 王李梦[1,2]

(1.西安理工大学教育部数控机床及机械制造装备集成重点试验室,西安710048,中国; 2.西安理工大学陕西省制造装备重点实验室,西安710048,中国)

摘要:设计了一种超磁致伸缩超声换能器,用有限元分析软件对理论设计的超声振动系统进行动力学分析,并对换能器进行了实验测试,验证了理论设计和仿真分析的正确性。为了研究导磁材料厚度对超磁致伸缩材料内磁场均匀度的影响规律,在超磁致伸缩棒与永磁体之间设置导磁材料,对换能器进行了磁场仿真分析。在对换能器进行阻抗分析和振幅测量基础上,对有无导磁材料时换能器的性能进行对比。实验结果表明:在超磁致伸缩材料与永磁体之间设置1.6 mm左右厚的导磁材料时,超磁致伸缩棒内的磁场均匀度最高;添加导磁材料后,超磁致伸缩换能器的输出振幅增大,机械品质因数减小,阻抗减小,使换能器工作更加稳定。

关键词:超磁致伸缩材料;超声换能器;磁场均匀度;有限元分析